JOURNAL OF SOLID STATE CHEMISTRY 33, 107–114 (1980)

Calorimetric Investigation of the Ferroelectric $\bar{4}3m$–$mm2$ Phase Transition in Boracite Crystals*

M. DELFINO,† G. M. LOIACONO, AND W. A. SMITH

Philips Laboratories, Briarcliff Manor, New York 10510

AND P. S. GENTILE

Fordham University, Bronx, New York 10458

Received February 23, 1979; in revised form August 8, 1979

The isobaric molar heat capacity of Cr–Cl, Fe–I, Cu–Cl, Ni–Br and Zn–Br boracite at the ferroelectric $\bar{4}3m$–$mm2$ phase transition is reported. The magnitude of the rise in C_p at the transition, and the large upper bound values of ΔH and ΔS prove that the phase transition is first order. The values of ΔH follow the trend Zn–Br $\gg$ Ni–Br > Cr–Cl $\gg$ Cu–Cl > Fe–I reflecting possible structural dissimilarities amongst the boracites. Thermal annealing of single crystal boracite samples of Ni–Br and Cr–Cl is found to remove multiple peaking of the heat capacity at the transition resulting in single peak heat capacity curves. The multiple peaking is thought to arise from internal stresses within the crystal.

Introduction

Boracites of the type $M_3B_7O_{13}X$, where M is a divalent metal and X is a monovalent anion, are generally characterized by a high-temperature paraelectric phase, space group $F\bar{4}3c$ (T_d^5), and a low-temperature ferroelectric phase, space group $Pca2_1$ (C_{2v}^5). The $\bar{4}3m$–$mm2$ ferroelectric phase transition is the subject of considerable interest (*1*) since it is thought to be an improper ferroelectric phase transition (*2, 3*), although alternative interpretations have been offered (*4, 5*).

To date, very little work has been reported on the thermodynamic nature of the $\bar{4}3m$–$mm2$ ferroelectric phase transition in boracites. Smutny (*6*) examined the heat capacity of Co–I boracite ($Co_3B_7O_{13}I$) and Schmid *et al.* (*7*) reported on the heat capacity of Fe–I boracite. Neither study examined the vicinity of the phase transition in detail, and the temperature dependence of the heat capacity was not explored in sufficient detail to make structural correlations. These studies did, however, show that the phase transition is strongly first order.

In view of the small amount of thermodynamic data available relative to the large number of boracites realizable, we examined the heat capacity of the $\bar{4}3m$–$mm2$ ferroelectric phase transitions in Cr–Cl, Fe–I, Cu–Cl, Ni–Br, and Zn–Br boracite. The results of this work and the effect of internal stresses upon the heat capacity at the phase transition are reported.

* Presented in part at the 4th American Conference on Crystal Growth, Gaithersburg, Md., July 16–19, 1978.

† Present address: Fairchild Research and Development Laboratory, Palo Alto, Calif. 94304.

0022-4596/80/070107-08$02.00/0

Experimental

1. Materials Origin and Characterization

The thermodynamic measurements were made on single crystals of Ni–Br, Cu–Cl, and Fe–I boracite obtained from F. W. Ainger and R. Whatmore (Plessey, England) and single crystals of Ni–Br and Fe–I boracite from T. Gier (DuPont). Single crystals of Cr–Cl and Zn–Br boracite were supplied by J. Kobayashi (Waseda University, Japan). All of these boracite samples were grown by the vapor transport method of Schmid (*8*). Powder samples of Ni–Br and Zn–Br boracite synthesized by a low-pressure/temperature hydrothermal method developed in this laboratory (*9*) were investigated also.

The chemical integrity of all of the boracite samples studied was verified by wet chemical analyses, infrared vibrational spectroscopy, electronic absorption spectroscopy, and X-ray diffraction. The results of this work will be published elsewhere.

2. Calorimetric Measurements

Calorimetric data were obtained with a Perkin–Elmer differential scanning calorimeter, model DSC-2, interfaced to a Textronix programmable calculator, model 31. The system is equipped with an Autoscan Zero mincomputer for automatic baseline corrections. The instrument was calibrated relative to the melting point and enthalpy of fusion of 5 *N* indium metal ($T_M = 429.87$ K and $\Delta H_f = 3266.8$ J mole^{-1}) and of 6 *N* lead metal ($T_M = 600.65$ K and $\Delta H_f = 4768.1$ J mole^{-1}). Both the melting points and the enthalpies of fusion were found to be independent of heating and cooling rates from 0.625 to 10 K min^{-1} and reproducible to ± 0.02 and ± 0.75, respectively.

Boracite samples were typically between 5 and 50 mg and were weighed with a precision of 1×10^{-4}. Open aluminum sample pans were employed as crucibles for single-crystal specimens. In all cases, the largest and flattest crystal facet of the sample was placed parallel to the bottom of the pan to ensure good thermal contact. For powder samples, the specimens were encased in the sample pan with an aluminum lid.

Quantitative heat capacity data were obtained in a heating mode only. Cooling curves were measured also but only used for qualitative comparison ith the heating curves. Over large temperature spans, e.g., 150 K, heat capacity data were obtained at integration intervals of 0.20 K and at heating rates of 2.5 K min^{-1}. In the vicinity of the phase transition, the integration interval was 0.078 K at a heating rate of 1.25 K min^{-1}. Thus, the fine detail of the heat capacity behavior at the phase transition could be clearly observed.

3. Temperature Annealing

Single crystal samples of Cr–Cl and Ni–Br boracite were wrapped in platinum foil suspended in an alumina crucible and heated in air in a sealed vertical tube furnace to 1100 ± 5 K. The temperature gradient was less than 1 K cm^{-1} across the samples. After a minimum soak time of 24 hr, the samples were cooled down at a constant rate of 12 K hr^{-1} to room temperature.

Results and Discussion

1. Temperature Dependence of the Heat Capacity

The temperature dependence of the isobaric (at atmospheric pressure) molar heat capacity of Cr–Cl, Fe–I, Cu–Cl, Ni–Br, and Zn–Br boracite in the *mm*2 and $\bar{4}3m$ crystal phases is given in 5 K intervals in Tables I–V. These data are the results of averaging at least two sets of measurements on two different samples from a given source and are further refined by normalization to the National Bureau of Standards heat capacity values for sapphire (*10*) corrected on a sapphire standard, measured under identical operating parameters. The sample to sample

variation was of the order of ±3%, whereas successive measurements on a given sample agreed to within ±0.8%. The heat capacities of powder samples of Ni–Br and Zn–Br boracite synthesized in our laboratory agree well with the measurements on the single-crystal samples of Ni–Br boracite (Plessey) and Zn–Br boracite (Wasseda University). Tables I–V report the single-crystal data, which are considered to be more reliable. The Ni–Br boracite (DuPont) gave heat capacity values as much as 5% smaller than those of the Plessey samples. The heat capacity of Fe–I boracite (DuPont) was typically 8% smaller in magnitude than that of the Plessey samples. The reason for these observed differences is not known to us and not reflected in any chemical analyses which we have performed.

It should be noted that these heat capacity measurements were performed under open circuit electrical boundary conditions ($\mathbf{E} \geq 0$). In a preliminary study of Fe–I boracite, we show that the heat capacity measured $\mathbf{E} \geq 0$) is identical to within ±0.8% of the heat capacity measured under closed circuit conditions ($\mathbf{E} = 0$) (*11*). This behavior is assumed to apply to the other boracites in this study.

TABLE I

ISOBARIC MOLAR HEAT CAPACITY OF Cr–Cl BORACITE IN THE *mm*2 AND $\bar{4}3m$ PHASES (MW = 475.12)

T (K)	C_p (J mole^{-1} K^{-1})	T (K)	C_p (J mole^{-1} K^{-1})
240.0	269.6±5.0	320.0	285.3
245.0	278.5	325.0	288.2
250.0	286.9	330.0	291.6
255.0	300.0	335.0	292.2
260.0	318.9	340.0	294.6
265.8	$\bar{4}3m$–*mm*2	345.0	297.0
	transition	350.0	299.2
270.0	260.6	355.0	303.2
275.0	262.8	360.0	306.7
280.0	265.2	365.0	310.1
285.0	268.4	370.0	312.5
290.0	271.3	375.0	315.1
295.0	272.5	380.0	317.3
300.0	274.7	385.0	318.1
305.0	278.1	390.0	319.3
310.0	280.7	395.0	320.1
315.0	283.1	400.0	321.4

TABLE II

ISOBARIC MOLAR HEAT CAPACITY OF Fe–I BORACITE IN THE *mm*2 AND $\bar{4}3m$ PHASES (MW = 578.10)

T (K)	C_p (J mole^{-1} K^{-1})	T (K)	C_p (J mole^{-1} K^{-1})
270.0	354.8±5.0	355.0	374.9
275.0	361.6	360.0	380.5
280.0	367.9	365.0	385.8
285.0	376.6	370.0	391.1
290.0	383.4	375.0	396.0
295.0	387.5	380.0	399.4
300.0	395.2	385.0	404.7
305.0	403.2	390.0	408.8
310.0	411.2	395.0	412.7
315.0	418.7	400.0	414.3
320.0	427.7	405.0	418.1
325.0	433.2	410.0	421.8
330.0	436.6	415.0	424.8
335.0	444.6	420.0	427.7
340.0	446.8	425.0	430.1
346.2	$\bar{4}3m$–*mm*2	430.0	432.7
	transition	435.0	435.2
350.0	372.0	440.0	436.9

In both crystal phases, the heat capacity of all the boracites increases monotonically with temperature. Using a least-squares curve fit of the refined data, we derive the temperature dependence of the isobaric molar heat capacity for the different boracites in the *mm*2 and $4\bar{3}m$ crystal phases over a limited temperature range. The resulting functions are given in Tables VI and VII. In the *mm*2 phase, the value of $\partial C_p/\partial T$ decreases as the molecular weight of the boracite increases. In the $4\bar{3}m$ phase, with the exception of Ni–Br boracite, we observe that the value of $\partial C_p/\partial T$ increases with an increase in the molecular weight of the boracite. The significance if any of these observations is not yet known.

TABLE III

ISOBARIC MOLAR HEAT CAPACITY OF Cu–Cl BORACITE IN THE *mm*2 AND $\bar{4}3m$ PHASES (MW = 509.75)

T (K)	C_p (J mole^{-1} K^{-1})	T (K)	C_p (J mole^{-1} K^{-1})
270.0	206.1 ± 5.0	365.0	427.8
275.0	216.5	369.7	$\bar{4}3m$–*mm*2
280.0	227.0		transition
285.0	237.2	375.0	425.7
290.0	248.9	380.0	392.9
295.0	259.9	385.0	391.2
300.0	270.8	390.0	393.5
305.0	281.2	395.0	397.3
310.0	292.4	400.0	399.1
315.0	302.8	405.0	403.1
320.0	313.6	410.0	306.7
325.0	323.1	415.0	409.7
330.0	337.0	420.0	412.9
335.0	341.7	425.0	415.9
340.0	351.3	430.0	418.5
345.0	370.0	435.0	421.4
350.0	372.0	440.0	423.0
355.0	390.9	445.0	424.4
360.0	407.4	450.0	425.9

TABLE IV

ISOBARIC MOLAR HEAT CAPACITY OF Ni–Br BORACITE IN THE *mm*2 AND $\bar{4}3m$ PHASES (MW = 539.70)

T (K)	C_p (J mole^{-1} K^{-1})	T (K)	C_p (J mole^{-1} K^{-1})
270.0	239.3 ± 5.0	375.0	410.5
275.0	247.5	380.0	417.3
280.0	255.6	385.0	425.7
285.0	263.8	390.0	428.1
290.0	271.8	395.0	503.5
295.0	280.0	398.4	$\bar{4}3m$–*mm*2
300.0	288.0		transition
305.0	296.1	405.0	467.2
310.0	304.5	410.0	415.5
315.0	312.3	415.0	417.3
320.0	320.3	420.0	420.0
325.0	328.5	425.0	423.2
330.0	336.7	430.0	425.7
335.0	344.9	435.0	429.0
340.0	353.0	440.0	430.6
345.0	361.1	445.0	432.7
350.0	369.1	450.0	434.5
355.0	377.1	455.0	436.0
360.0	385.0	460.0	437.4
365.0	393.8	465.0	439.2
370.0	401.7	470.0	440.6

*2. The Ferroelectric $\bar{4}3m$–*mm*2 Phase Transition*

The detailed heat capacity curves of Cr–Cl, Fe–I, Cu–Cl, Ni–Br, and Zn–Br boracite in the vicinity of the phase transition are shown in Figs. 1–5. The thermodynamic values computed from these curves are given in Table VIII. The transition temperature T_c is taken as the peak in the heat capacity. Our T_c values for Fe–I, Cu–Cl, Ni–Br, and Zn–Br boracite are in excellent agreement with the work of Schmid (*8*). However, for Cr–Cl boracite, we observe a T_c of 265.8 ± 0.2 K, whereas Schmid (*8*) finds 251–257 K. This discrepancy can be attributed to the partial substitution of OH for Cl in the Cr–Cl sample of Schmid (*8*) since our samples did not show any evidence of OH substitution at a level of 0.5%. The thermal hysteresis, ΔT, refers to the displacement of T_c to a lower temperature recorded on cooling through the phase

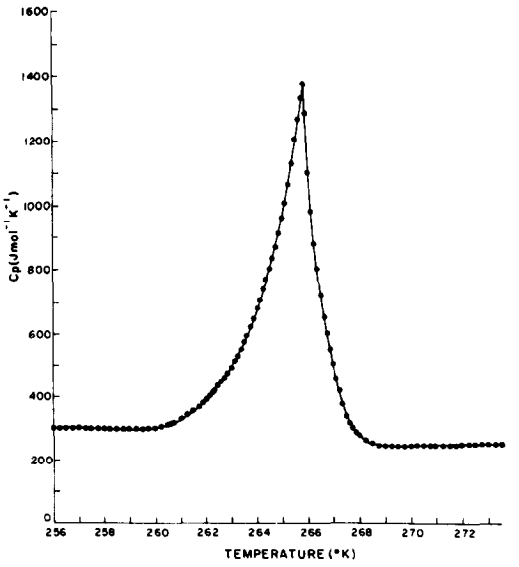

FIG. 1. Isobaric molar heat capacity of Cr–Cl boracite in the vicinity of the $\bar{4}3m$–*mm*2 phase transition.

TABLE V

ISOBARIC MOLAR HEAT CAPACITY OF Zn-Br BORACITE IN THE $mm2$ AND $\bar{4}3m$ PHASES (MW = 559.71)

T (K)	C_p (J mole^{-1} K^{-1})	T (K)	C_p (J mole^{-1}) K^{-1})
455.0	401.7 ± 5.0	555.0	551.7
460.0	409.2	560.0	559.2
465.0	416.7	565.0	566.8
470.0	424.5	570.0	574.2
475.0	431.8	575.0	581.7
480.2	439.2	584.6	$\bar{4}3m$–$mm2$
485.0	436.5		transition
490.0	454.2	590.0	585.2
495.0	461.8	595.0	588.5
500.0	469.2	600.0	592.1
505.0	476.8	605.0	595.3
510.0	484.1	610.0	599.0
515.0	491.5	615.0	602.1
520.0	499.0	620.0	605.6
525.0	506.7	625.0	609.0
530.0	514.5	630.0	612.5
535.0	521.7	635.0	615.5
540.0	529.0	640.0	619.0
545.0	536.7	645.0	622.5
550.0	544.0	650.0	625.9

transition. The enthalpy of transition ΔH is obtained by integrating the area under the heat capacity curve within the limits of a constructed baseline which spans the initial heat capacity rise to the heat capacity descent in the high-temperature phase. This is shown schematically in Fig. 6. The entropy of transition ΔS is obtained by dividing ΔH by T_c. This approximation assumes that the transition occurs over a small enough temperature interval, i.e., ~8 K, so that the error in this approximation is negligible. Thus the values of ΔH and ΔS are upper bounds on the true latent heat and excess entropy at the transition.

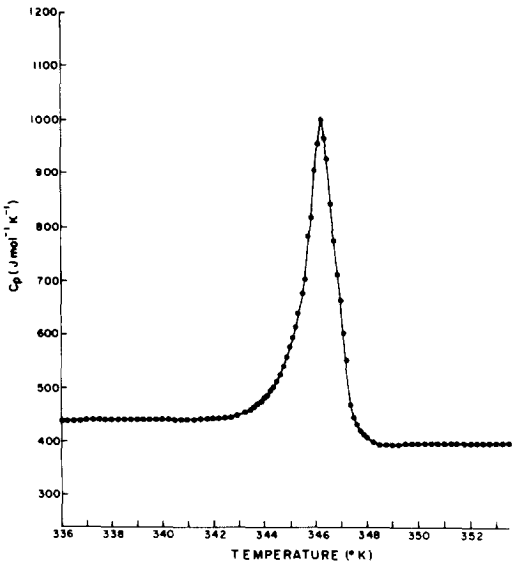

FIG. 2. Isobaric molar heat capacity of Fe–I boracite in the vicinity of the $\bar{4}3m$–$mm2$ phase transition.

Schmid *et al.* (*7*) previously reported the heat capacity of Fe–I boracite measured also by differential scanning calorimetry. Their results are generally in good agreement with ours, except for a serious discrepancy concerning the magnitude of the enthalpy of transition. They observe $\Delta H = 3100 \pm 300$ J mole^{-1}, whereas we find

TABLE VI

LEAST-SQUARES FIT OF THE ISOBARIC MOLAR HEAT CAPACITY FUNCTIONS FOR BORACITES IN THE $mm2$ PHASE

Boracite	Temperature interval	C_p (J mole^{-1} K^1)
Cr–Cl	$240 \leq T(K) \leq 260$	$-3.097\times10^2+24.0\times10^{-1}T$
Fe–I	$270 \leq T(K) \leq 340$	$-0.157\times10^2+13.7\times10^{-1}T$
Cu–Cl	$270 \leq T(K) \leq 355$	$-3.776\times10^2+21.6\times10^{-1}T$
Ni–Br	$270 \leq T(K) \leq 385$	$-1.986\times10^2+16.2\times10^{-1}T$
Zn–Br	$455 \leq T(K) \leq 575$	$-1.849\times10^2+15.0\times10^{-1}T$

TABLE VII

LEAST-SQUARES FIT OF THE ISOBARIC MOLAR HEAT CAPACITY FUNCTIONS FOR BORACITES IN THE $\bar{4}3m$ PHASE

Boracite	Temperature interval	C_p (J mole^{-1} K^{-1})
Cr–Cl	$270 \leq T(K) \leq 400$	$1.374\times10^{2}+4.588\times10^{-1}T$
Fe–I	$350 \leq T(K) \leq 440$	$1.184\times10^{2}+7.353\times10^{-1}T$
Cu–Cl	$385 \leq T(K) \leq 450$	$1.741\times10^{2}+5.654\times10^{-1}T$
Ni–Br	$410 \leq T(K) \leq 470$	$2.411\times10^{2}+4.279\times10^{-1}T$
Zn–Br	$590 \leq T(K) \leq 650$	$1.849\times10^{2}+6.784\times10^{-1}T$

$\Delta H = 1005 \pm 50$ J mole^{-1}. This discrepancy is not readily explained. However, reintegrating their heat capacity curve results in a ΔH of the order of 1500 J mole^{-1}.

Several interesting conclusions can be made from these thermodynamic data. The magnitude of the peak in C_p, the large value of ΔH and ΔS, and the somewhat small value of ΔT show that the ferroelectric $\bar{4}3m$–$mm2$ phase transition is first order. From X-ray diffuse scattering experiments, Felix *et al.* (*12*) conclude that the first-order character of the phase transition decreases with a decrease in the mass and size of the halogen. Using our ΔH values as a measure of the first-order character, we observe the trend Zn–Br ≫ Ni–Br > Cr–Cl ≫ Cu–Cl > Fe–I. The anomalously large ΔH value measured for Zn–Br boracite suggests that more than the halogen is responsible for the first-order character of the transition. Although these boracites are reported to be isostructural, this observation suggests possible structural dissimilarities, reflecting different metal site symmetries or different boron–oxygen

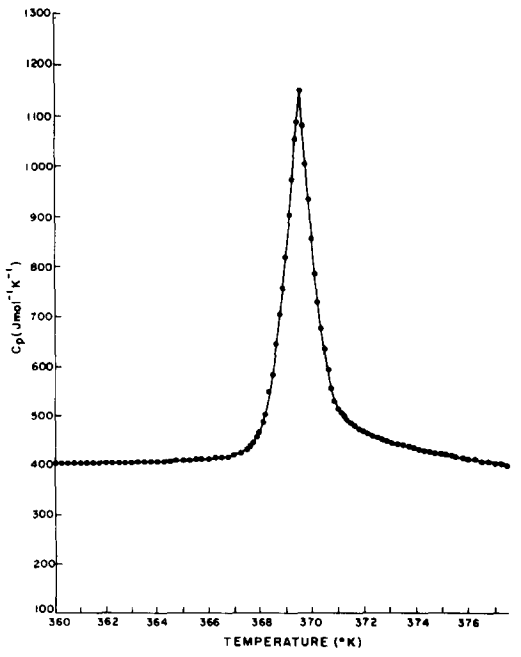

FIG. 3. Isobaric molar heat capacity of Cu–Cl boracite in the vicinity of the $\bar{4}3m$–$mm2$ phase transition.

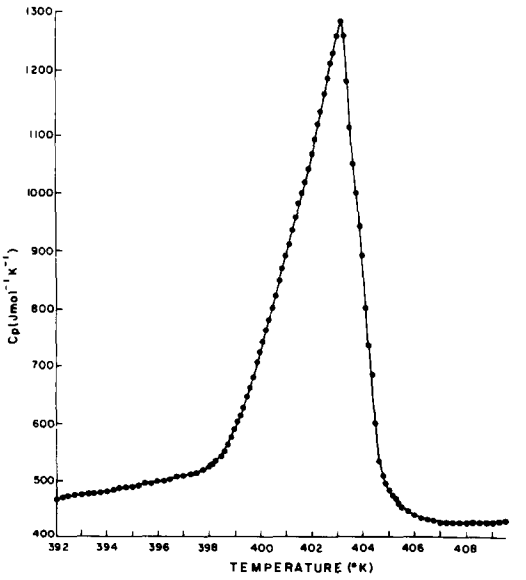

FIG. 4. Isobaric molar heat capacity of Ni–Br boracite in the vicinity of the $\bar{4}3m$–$mm2$ phase transition.

TABLE VIII

THERMODYNAMIC VALUES FOR THE $\bar{4}3m$–$mm2$ PHASE TRANSITION IN BORACITE CRYSTALS

Boracite	T_c (K)	ΔT (K)	ΔH (J mole^{-1})	ΔS (J mole^{-1} K^{-1})
Cr–Cl	265.8±0.2	1.2±0.4	2145±110	8.07±0.45
Fe–I	346.2±0.2	2.4±0.4	1005±50	2.90±0.15
Cu–Cl	369.7±0.2	2.7±0.4	1220±60	3.30±0.20
Ni–Br	398.4±0.2	1.6±0.4	2845±150	7.14±0.40
Zn–Br	584.6±0.2	3.2±0.4	4275±200	7.31±0.35

frameworks. This is consistent ith the suggestion of Nelmes (*1*), who distinguishes at least three types of orthorhombic boracite based on available X-ray structural data.

3. Multiple Peaking of the Heat Capacity at the Transition

During the course of this investigation, some boracite samples were observed to exhibit multiple peaking of the heat capacity at the phase transition. The heat capacity at the transition of crystals of Cr–Cl and Ni–Br boracite were always multiple peaked, whereas the heat capacities of Fe–I and Ni–Br boracite were more often single peaked than multiple peaked. No samples of Cu–Cl boracite were observed to exhibit multiple-peaked heat capacities. Extreme examples of multiple peaking in the heat capacity of Cr–Cl and Ni–Br boracite are shown in Figs. 7 and 8, respectively. The number of heat capacity peaks and their general shape are not characteristic of any particular boracite type. Successive measurements made on a given sample of either boracite were reproducible with only small fluctuations (e.g., $<10\%$) occurring in the various heat capacity peaks.

It is proposed that the multiple peaking of the heat capacity is due to internal stresses in the boracite crystal. These internal stresses

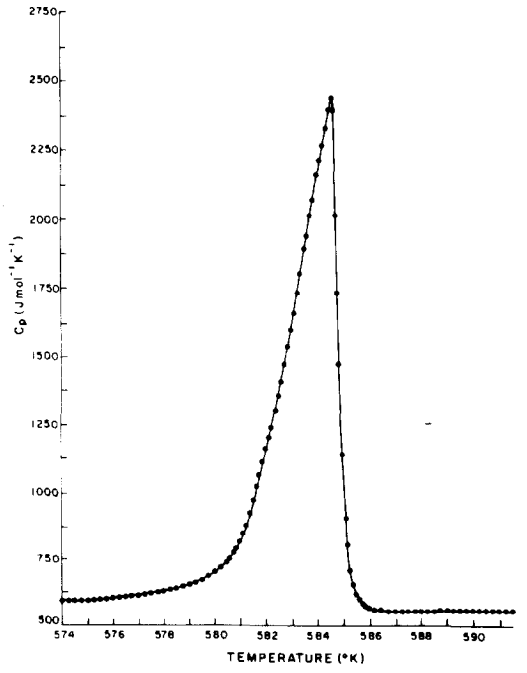

FIG. 5. Isobaric molar heat capacity of Zn–Br boracite in the vicinity of the $\bar{4}3m$–$mm2$ phase transiton.

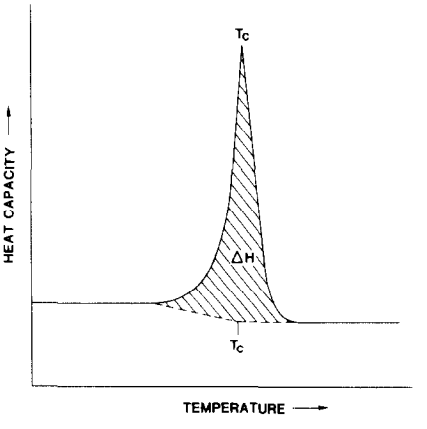

FIG. 6. Schematic representation of method of integration for determining ΔH.

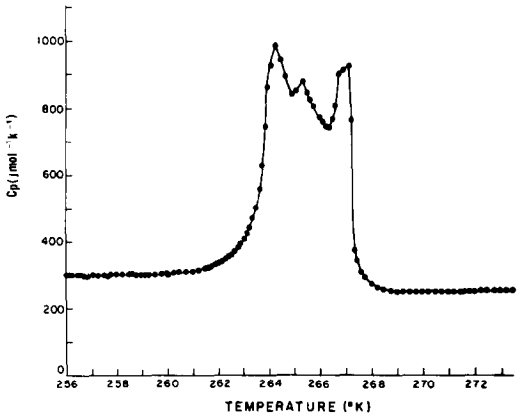

FIG. 7. Multiple peaking of the isobaric molar heat capacity of Cr–Cl boracite at the $\bar{4}3m$–$mm2$ phase transition.

cause shifts of the transition temperature so that the phase transition occurs at different points in the crystal at slightly different temperatures. If this is indeed the origin of the multiple peaking, thermal annealing of the samples would relieve the internal stresses resulting in a heat capacity with a single peak. Heat capacity measurements performed on thermally annealed samples which previously were multiple peaked showed single peaks in the heat capacity. Some samples did, however, show some evidence of residual multiple peaking even after thermal annealing. The resulting single-peak heat capacity samples (Figs. 1 and 4) have been discussed.

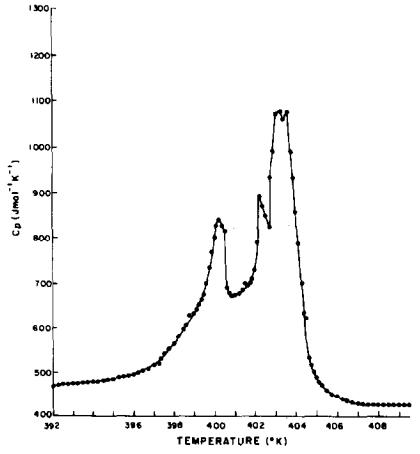

FIG. 8. Multiple peaking of the isobaric molar heat capacity of Cr–Cl boracite at the $\bar{4}3m$–$mm2$ phase transition.

If we compare the multiple-peaked samples to the single-peak samples of Cr–Cl and Ni–Br boracite, we observe that the transition is spread out when multiple peaking occurs. The values of ΔH for the multiple-peaked heat capacity curves in Cr–Cl and Ni–Br boracite are 1146 ± 110 and 2600 ± 125 J mole^{-1}, respectively. These are in good agreement with the ΔH values of the single-peaked heat capacity samples: Cr–Cl, $\Delta H = 1145 \pm 110$ J mole^{-1}, and Ni–Br, $\Delta H = 2845 \pm 150$ J mole^{-1}.

It appears from these results that multiple peaking of the heat capacity in boracites arises from internal stresses. Thermal annealing relieves these internal stresses resulting in single-peak heat capacity curves.

Acknowledgments

This research was sponsored by USAECOM, Night Vision and Electro-Optics Laboratories under Government Contract DAAG53-76-C-0053. The authors thank F. W. Ainger, R. Whatmore, T. Gier, and J. Kobayashi for the boracite samples used in this study.

References

1. R. J. NELMES, *J. Phys. C: Solid State Phys.* **7**, 3840 (1974).
2. V. DVORAK AND J. PETZELT, *Czech. J. Phys. B* **21**, 11441 (1971).
3. V. DVORAK, *Czech. J. Phys. B* **21**, 1250 (1971).
4. YU. M. GUFAN AND V. P. SAKHNENKO, *Sov. Phys. Solid State* **14**, 1660 (1973).
5. A. P. LEVANYUK AND D. G. SANNIKOV, *Sov. Phys. Solid State* **17**, 327 (1975).
6. F. SMUTNY, *Phys. Status Solidi A* **9**, K109 (1972).
7. H. SCHMID, P. CHAN, L. A. PETERMANN, F. TEUFEL, AND M. MANDLY, *Ferroelectrics* **13**, 351 (1976).
8. H. SCHMID, *J. Phys. Chem. Solids* **26**, 973 (1965).
9. M. DELFINO AND P. S. GENTILE, to be published.
10. D. C. GINNINGS AND G. T. FURUKAWA, *J. Amer. Chem. Soc.* **75**, 522 (1953).
11. M. DELFINO AND P. S. GENTILE, to be published.
12. P. FELIX, M. LAMBERT, R. COMES, AND H. SCHMID, *Ferroelectrics* **7**, 131 (1974).